Revista Mexicana de Astronomía y Astrofísica, **60**, 381–396 (2024)

https://doi.org/10.22201/ia.01851101p.2024.60.02.16

THE VARIABLE STARS POPULATION OF THE EXTENDED YOUNG GLOBULAR CLUSTER NGC 1851

A. Arellano Ferro[1], C. E. Pérez Parra[2,3], M. A. Yepez[4,5], I. Bustos Fierro[6], Z. Prudil[7], and L. J. Zerpa Guillen[2,3]

Received July 15 2024; accepted August 15 2024

ABSTRACT

We report *VI* CCD photometry of the globular cluster NGC 1851. We aim to study the membership of the variable stars detected in the field of the cluster as listed in the *Catalogue of Variable stars in Globular Clusters* (CVSGC; Clement et al. 2001) and reported by the *Gaia* mission. We cross match the two sets of variables to produce light curves that lead to the estimation of physical parameters. The resulting colour-magnitude diagram (CMD), free of likely field stars, enables us to confirm from the position of the variables their type and evolutionary stage. We provide new estimations of the period using data acquired on a long time-base. The Fourier decomposition of cluster member RR Lyrae light curves lead to a mean metallicity and distance of $[Fe/H]_{ZW} = -1.35 \pm 0.22$ dex and 11.9 ± 0.6 kpc. The variability and membership of stars reported by *Gaia*-DR3 as variables in the field of the cluster is discussed.

RESUMEN

Reportamos fotometría *VI* del cúmulo globular NGC 1851. La finalidad es hacer un análisis de membresía de las variables detectadas en el campo del cúmulo y reportadas en el *Catalogue of Variable stars in Globular Clusters* (CVSGC, Clement et al. 2001) y por la misión *Gaia*. Los dos conjuntos de datos permitieron la producción de curvas de luz y la estimación de parámetros físicos estelares. El diagrama color-magnitud resultante, sin estrellas de campo, permite confirmar el tipo de cada estrella variable y su estado evolutivo. Reportamos nuevas estimaciones de los periodos de pulsación. La descomposición de Fourier de las curvas de luz de estrellas RR Lyrae miembros del cúmulo conduce a los valores medios de la metalicidad y la distancia del cúmulo; $[Fe/H]_{ZW} = -1.35 \pm 0.22$ dex y 11.9 ± 0.6 kpc. Se discute la variabilidad y la membresía de las estrellas reportadas como variables por *Gaia*-DR3 en el campo del cúmulo.

Key Words: globular clusters: general — globular clusters: individual: NGC 1851 — stars: distances — stars: fundamental parameters — stars: horizontal branch — stars: variables: RR Lyrae

1. INTRODUCTION

The southern globular cluster NGC 1851 is a remarkably bright system located in the constellation Columba, and in the outer region of the Milky Way, at a distance of about 12.0 kpc from the Sun ($\alpha = 5^h14^m06.76^s$, $\delta = -40^o02'47.6''$, J2000; $l = 244.51^o$, $b = -35.03^o$). It is a highly concentrated system (Kuzma et al. 2018) characterized by a diffuse halo extending to more than 10 times the tidal radius, although according to Marino et al. (2014), stars dynamically linked to the cluster are present to at least 2.5 tidal radii. The Galactic orbit of

[1]Instituto de Astronomía, Universidad Nacional Autónoma de México, México.
[2]Universidad de Los Andes, Facultad de Ciencias, Dpto. Física, Grupo de Astrofísica Teórica, Mérida, Venezuela.
[3]Fundación Centro de Investigaciones de Astronomía Francisco, J. Duarte (CIDA), Mérida, Venezuela.
[4]Instituto Nacional de Astrofísica, Óptica y Electrónica, Tonantzintla, Puebla, México.
[5]Consejo Nacional de Humanidades, Ciencias y Tecnologías, Ciudad de México, México.
[6]Observatorio Astronómico, Universidad Nacional de Córdoba, Córdoba, Argentina.
[7]European Southern Observatory, Garching, Germany.

the cluster is very eccentric, $e = 0.7$, and the lack of a tidal tail has triggered the suggestion that the cluster may be a stripped dwarf galaxy nucleus accreted by the Milky Way (Kuzma et al. 2018). However, a tail that seems to emerge from NGC 1851 was detected by Carballo-Bello et al. (2018), which may be interpreted as a tidal remnant of a tentative progenitor dwarf galaxy host of NGC 1851. Its rather young age, 9.2 Gyr according to Koleva et al. (2008) or 11.0 Gyr according to VandenBerg et al. (2013), seems to support the hypothesis of an extra Galactic origin. From a chemo-dynamical analysis, Callingham et al. (2022) associated NGC 1851 to the ancient major merger event of the Milky Way Gaia-Enceladus-Sausage (Belokurov et al. 2018; Helmi et al. 2018).

The horizontal branch (HB) of NGC 1851 possesses a moderate population of hot blue tail stars and a dense red clump nearly twice as populated; hence its HB structural parameter $L = -0.36$ (Arellano Ferro 2024) is consistent with its Oosterhoff type Oo I and metallicity [Fe/H]=-1.3, following the trend defined by other Galactic clusters of the same Oo-type and similar metallicity.

NGC 1851 harbours a large number of RR Lyrae stars, 48 according the the 2020 edition of the *Catalogue of Variable Stars in Globular Clusters* (CVSGC, Clement et al. 2001). It may also contain 4-5 long period variables near the tip of the red giant branch (RGB). One of our goals in this paper is to employ the variable stars as indicators of the mean metallicity and distance of the parental cluster; hence it is of relevance to ask whether all the variables reported in the CVSGC are cluster members, since the large majority of them were discovered before a detailed membership analysis was a feasible possibility. In the present paper we propose a membership analysis based on the *Gaia*-DR3 proper motions before we produce a cleaner colour-magnitude diagram (CMD) and then to study the distribution of the variables and their physical properties.

2. OBSERVATIONS AND IMAGE REDUCTIONS

2.1. *Observations*

The *VI* CCD images were obtained with the 1.54m telescope of the Estación Astrofísica Bosque Alegre del Observatorio de Córdoba, Universidad Nacional de Córdoba, Argentina (EABA), during December 14, 15 and 16, 2018 and during five nights between April 6-28 2019. We shall refer to these seasons as BA18 and BA19 respectively. During the BA18 season we used the camera Alta F16M, equipped with a KAF-16803 chip of 4096×4096 square pixels of 9 microns, binned 2×2. This produced a scale of 0.496 arc seconds per pixel and resulted in a field of view of 16.9×16.9 square arc minutes. During the BA19 season the camera was an Alta U9 with a KAF-6303E CCD detector of 3072×2048 square pixels of 9 microns, also binned 2×2. The scale is 0.496 arc seconds per pixel for a field of view of 12.7×8.5 square arc minutes.

TABLE 1

LOG OF OBSERVATIONS OF NGC 1851

Date	N_V	t_V(s)	N_I	t_I(s)	Mean seeing ($''$)
2018-12-14	53	100	61	50	3.3
2018-12-15	72	100	80	50	2.3
2018-12-16	62	100	63	50	2.7
2019-04-06	13	100	13	50	3.4
2019-04-07	24	100	29	50	2.4
2019-04-12	23	100	24	50	2.5
2019-04-13	23	100	24	50	2.7
2019-04-28	23	100	24	50	2.6
Total:	293		318		

Columns N_V and N_I give the number of images taken with the V and I filters respectively. Columns t_V and t_I provide the exposure time. In the last column the prevailing nightly average seeing is listed.

The log of the observations is given in Table 1, where the employed exposure times and the nightly seeing conditions are indicated. The goal of these observations is to extract accurate photometry of all point sources in the field of our images, and to build their corresponding light curves. For this purpose we employed the difference imaging analysis (DIA) and the DanDIA pipeline (Bramich 2008; Bramich et al. 2013, 2015).

2.2. *Locking Our Photometry to the Standard System*

For the BA18 season we were able to produce light curves for 4623 point sources in the V-band and 1578 in the I-band. For the BA19 season we measured 2305 light curves in the V-band and 1949 in the I-band. These instrumental light curves were transformed to the standard Johnson-Kron-Cousins system defined by Landolt (1992), by employing the local standard stars in the field of NGC 1851 provided in the catalogue of Stetson (2000)[8]. We identified 179 and 101 standards in BA18 and BA19 respectively for which we have *VI* photometry. Figure 1 shows the dependence of the standard minus instrumental magnitudes with the instrumental colour $(v-i)$, from which the transformation equations, inscribed in the figure legend, were calculated. These

[8] https://www.canfar.net/storage/list/STETSON/Standards.

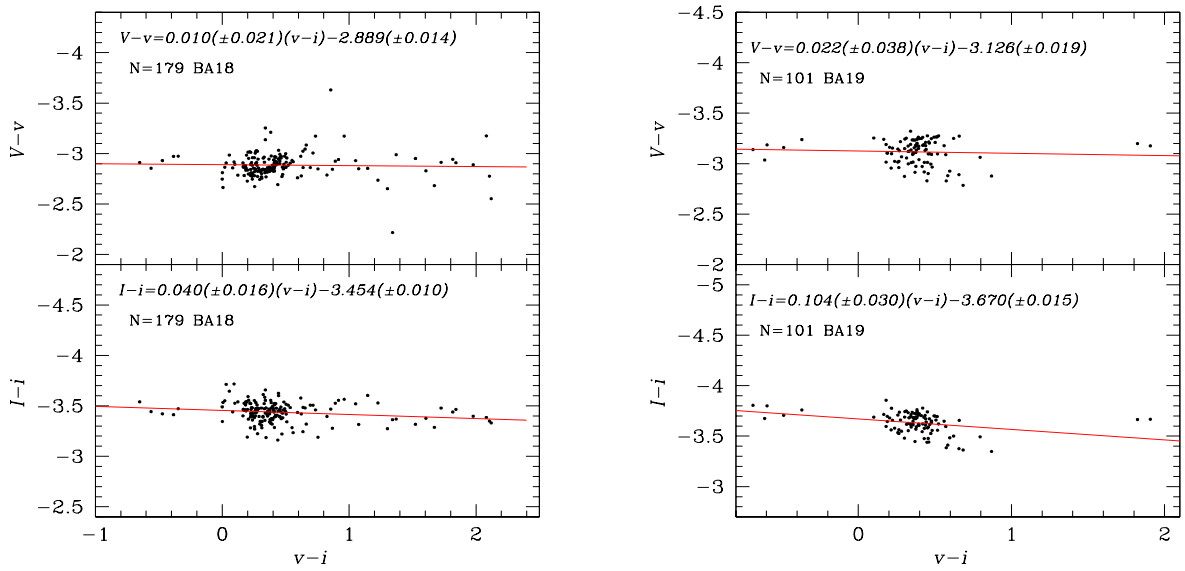

Fig. 1. Transformation relationship between *VI* instrumental and standard photometric systems, calculated for the BA18 and BA19 seasons with 179 and 101 standards respectively, taken from the collection of Stetson (2000).

equations were employed to convert all instrumental light curves into the standard system.

Table 2 displays a small portion of the time-series *VI* photometry obtained in this work. The full table will be made available in electronic form in the Centre de Donnés Astronomiques de Strasbourg database (CDS).

3. VARIABLE STARS IN THIS STUDY

We were able to measure *VI* magnitudes for 1434 stars identified as cluster members in the field of our images. These cluster members will be used to produce the CMD diagram. We could measure 47 of the 55 variables in the cluster listed by Clement et al. (2001) in the CVSGC. As can be seen in Table 1, the observations were carried out under limited seeing conditions, and as a result our DIA analysis was unable to retrieve useful data for stars that are very faint, stars near the cluster center, or stars blended with a brighter neighbour. We could not measure the RRab stars V30, V36, V39, V40, V41, V43 and V44.

From an independent exploration we detected clear variability of three faint stars that we temporarily call F1, F2 and F3.

The *Gaia*-DR3 lists 22 variable stars in the field of the cluster that do not match any of the V55 already known in the CVSGC. *Gaia* photometry is available for 21 of these stars. For the sake of clarity we list these 21 stars in Table 3 along with their *Gaia* source identification and equatorial coordinates. We arbitrarily number these variables with a prefix 'G'. We explore their light curves from our own photometry and from *Gaia* data, and can confirm with confidence the variability and nature for only five of them.

All the reported variables in field of NGC 1851 are listed in Table 4, along with their variable types,

TABLE 2

TIME-SERIES *VI* PHOTOMETRY FOR THE VARIABLE STARS OBSERVED*

Variable Star ID	Filter	HJD (d)	$M_{\rm std}$ (mag)	$m_{\rm ins}$ (mag)	σ_m (mag)
V1	*V*	2458467.53771	16.000	18.889	0.014
V1	*V*	2458467.55788	16.097	18.985	0.009
⋮	⋮	⋮	⋮	⋮	⋮
V1	*I*	2458467.53148	15.433	18.884	0.020
V1	*I*	2458467.53416	15.525	18.976	0.012
⋮	⋮	⋮	⋮	⋮	⋮
V3	*V*	2458467.53771	16.264	19.155	0.019
V3	*V*	2458467.55788	16.206	19.097	0.012
⋮	⋮	⋮	⋮	⋮	⋮
V3	*I*	2458467.53148	15.719	19.179	0.026
V3	*I*	2458467.53416	15.775	19.235	0.018
⋮	⋮	⋮	⋮	⋮	⋮

*The standard and instrumental magnitudes are listed in Columns 4 and 5, respectively, corresponding to the variable stars in Column 1. Filter and epoch of mid-exposure are listed in Columns 2 and 3, respectively. The uncertainty in $m_{\rm ins}$, which also corresponds to the uncertainty in $M_{\rm std}$, is listed in Column 6. A full version of this table is available at the CDS database.

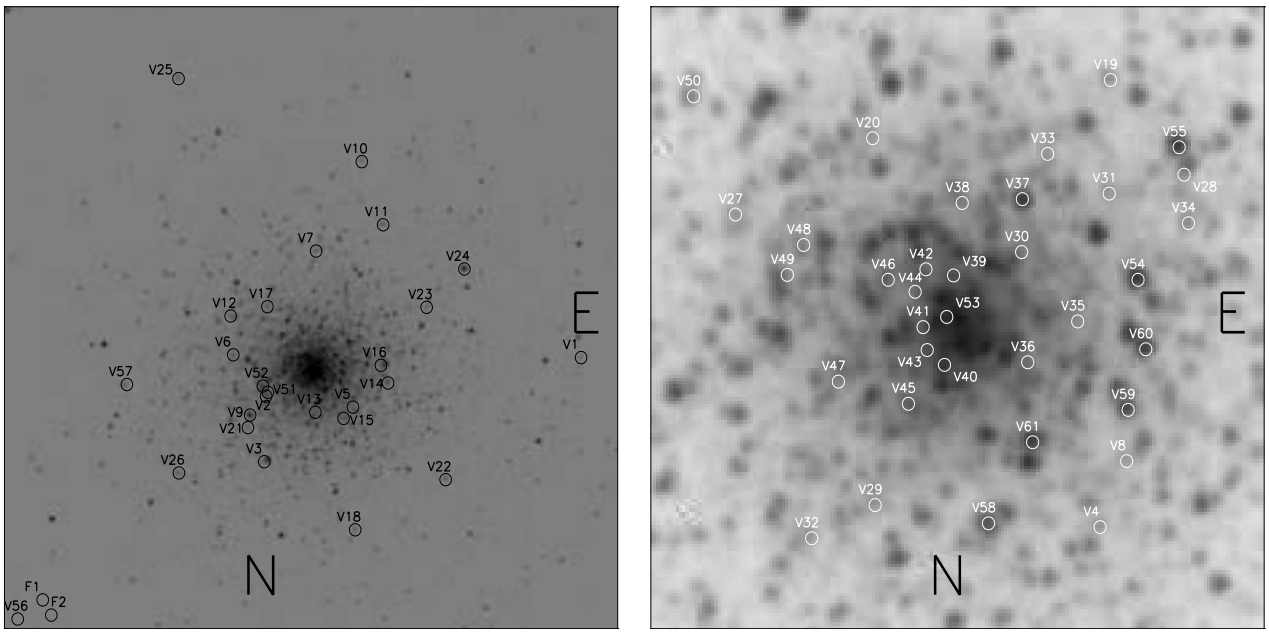

Fig. 2. Identification chart of variable stars in the field of NGC 1851. The approximate size of the images is 9.7×9.7 and 1.6×1.6 square arc minutes.

mean magnitudes, amplitudes and ephemerides whenever possible. Included in the table are also the stars that we were unable to measure and the non-confirmed *Gaia* variables, since we are providing their equatorial coordinates and a proper field identification.

The cluster membership status of all these variables is discussed in the following section.

We offer a finding chart of all the variables in Figure 2. Their light curves are displayed in the Appendix, where we shall distinguish the data from different seasons. In the Appendix we also discuss individual peculiar or outstanding variables.

4. STELLAR MEMBERSHIP ANALYSIS

In current times, the membership analysis of large numbers of stars in the field of a given globular cluster is possible thanks to the high quality of proper motions available in the *Gaia* mission (Gaia Collaboration et al. 2023). Sieving the likely cluster members and the field stars, enables the production of cleaner CMDs, and hence a better perspective of the stellar distributions and evolutionary properties. This is of particular interest for specific groups of variable stars, e.g. RR Lyrae stars in the horizontal branch (HB).

The method developed by Bustos Fierro & Calderón (2019) to determine the stellar membership is based on a two step approach: (1) it finds groups of stars with similar characteristics in the four-dimensional space of the gnomonic coordinates ($X_{\rm t}$,$Y_{\rm t}$) and proper motions ($\mu_{\alpha*}$,μ_{δ}) employing the Balanced Iterative Reducing and Clustering using Hierarchies (BIRCH) clustering algorithm (Zhang et al. 1996); and (2) in order to extract likely members that were missed in the first stage, the analysis of the projected distribution of stars with different proper motions around the mean proper motion of the cluster is performed.

Figure 3 shows the corresponding vector point diagram (VPD) and CMD, distinguishing the likely cluster members from the field stars. We considered a 30 arc minute radius field from the cluster center, which contains 25238 *Gaia* point sources out of which 11220 were found to be likely cluster members.

An independent membership analysis for a large number of globular clusters, based on the proper motions of *Gaia*-DR3, was performed by Vasiliev & Baumgardt (2021). These authors provided membership probabilities for each star in the cluster field. In Columns 9 and 10 of Table 4 we list the membership status according the method from Bustos Fierro & Calderón (2019) (B&C) and the probabilities from Vasiliev & Baumgardt (2021) (V&B). With a few exceptions, the match is good. The exceptions that call for attention are V8, V25, V37, V42, V44, V45 and V48, and their membership status deserves a few comments. We should note that the coordi-

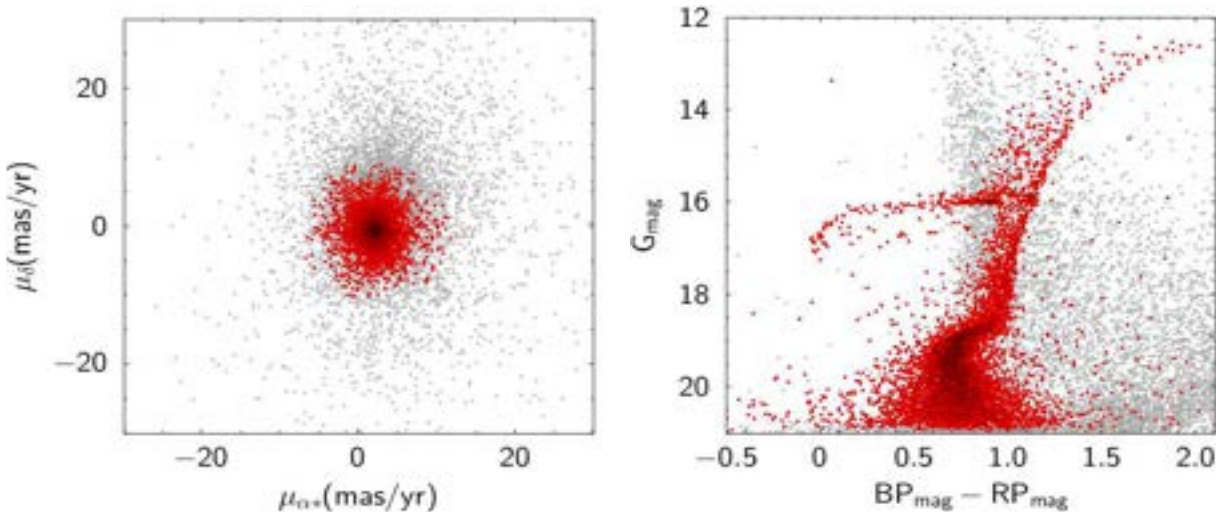

Fig. 3. *Gaia*-DR3 VPD (left panel) and CMD (right panel) of the cluster NGC 1851. Red and gray points correspond to likely cluster members and field stars, respectively, determined as described in § 4. A total of 25238 *Gaia* point sources within 30 arc minutes are displayed, while 11220 were found to be cluster members. The colour figure can be viewed online.

TABLE 3

VARIABLE STARS IN THE FIELD OF NGC 1851 REPORTED IN *GAIA*-DR3

Var Id	*Gaia* Source	R.A.	DEC
G1	4819198634647024512	05:14:02.32	-40:00:01.0
G2	4819198187968154496	05:13:52.49	-40:01:04.3
G3	4819198089187642112	05:13:51.14	-40:02:37.2
G4	4819197779947169152	05:14:02.37	-40:01:41.9
G5	4819197779945787392	05:14:00.84	-40:01:38.4
G6	4819197711229437952	05:14:05.02	-40:01:51.9
G7	4819197676868199168	05:14:01.50	-40:02:37.9
G8	4819197608151761152	05:14:08.52	-40:01:55.8
G9	4819197608147820032	05:14:11.79	-40:02:09.2
G10	4819197505072742912	05:14:07.05	-40:02:18.2
G11	4819197505072715264	05:14:08.96	-40:02:35.0
G12	4819197505072513152	05:14:05.82	-40:02:46.2
G13	4819197500774037376	05:14:09.21	-40:02:44.2
G14	4819197500774029312	05:14:07.67	-40:02:30.3
G15	4819197500774029056	05:14:07.64	-40:02:27.0
G16	4819197470714194304	05:14:02.92	-40:03:30.8
G17	4819197436349844992	05:14:08.95	-40:03:40.1
G18	4819197401991836544	05:14:06.29	-40:03:59.8
G19	4819197092756042496	05:14:01.95	-40:04:41.6
G20	4819185822760255616	05:14:19.10	-40:02:26.4
G21	4819185685319251456	05:14:13.34	-40:04:12.9

nates given in the CVSGC are the starting point for a match with *Gaia* and that for stars V37, V38, V42, V45, V46 and V48 only X,Y coordinates are listed; hence the matching is sometimes more dubious. In the present work we provide equatorial coordinates for these six stars

We should consider the fact that at the reported coordinates in Table 4, we recover in our photometry the light curve of a variable star of the expected type, period and light curve morphology, and that their position in the CMD also becomes a sound membership indicator tool. Therefore, we conclude that V8 is a cluster member, whereas V25, based on its accurate parallax is a field star, much closer than the cluster. For RR Lyrae stars V37, V42, V45, V47, V48, V50 and V53 there are good matches with *Gaia* sources with good proper motions, but in all cases the corresponding stars are much brighter than the HB, as can be appreciated in the CMD; hence they are all foreground field RR Lyrae stars. Given that at least one of the two membership identification methods indicate that they are field stars, we opted for labeling them as such. Similarly off the HB there are the RR Lyrae V14, V33, and V51. However in these cases both B&C and V&B approaches identify them as very likely cluster members. Since these are located near the central region of the cluster, we cannot rule out contamination of our photometry by close unresolved neighbours and we opted for considering them likely cluster members. We were unable to reliably measure the star V44 in the central region of the cluster, and hence its membership status remains unknown (UN).

Regarding the variable stars reported by *Gaia*-DR3, listed in Table 3, all but G17, G18 and G21 were found to be cluster members by both B&C and V&B. All stars marked with 'UN' by B&C lack proper motion in the *Gaia* database; hence its membership cannot be assessed from that information. In

Column 11 of Table 4 we list our final membership assessment.

4.1. *The New Variables in the Field of NGC 1851*

Of the three newly detected variables in the field of NGC 1851, F1, F2 and F3, only F3 is a likely cluster member; hence we assigned to it the variable number V56 and we tentatively classified it as SX Phe star. These three stars are contained in Table 4, and their light curves are displayed in the Appendix.

5. THE OOSTERHOFF TYPE OF NGC 1851

The period averages for the RRab and RRc stars in NGC 1851 are $<P\mathrm{ab}> = 0.57 \pm 0.06$ days and $<P\mathrm{c}> = 0.31 \pm 0.04$ days. These numbers point to an Oosterhoff type Oo I for this cluster. In the $\log P$ - amplitude plane, or Bailey's diagram, of Figure 4 we plot amplitudes and periods for all RR Lyrae stars measured in the this work (Table 4). The distribution of star on this plane clearly favours the unevolved sequences and the Oo I type of this cluster, in agreement with the average periods and the metallicity of the cluster of about $[\mathrm{Fe/H}]_{\mathrm{UV}} = -1.25$, (see § 7).

6. ON THE CLUSTER REDDENING

Given its Galactic location, the reddening of NGC 1851 is relatively low compared to other globular clusters closer to the Galactic plane, where the density of dust and gas is higher. Independent estimates of the cluster reddening consistently report low values of $E(B-V)$; for example, Harris (1996) and Walker (1998) give a value of $E(B-V) = 0.02$. The latter stresses that there are no compelling evidences for values too different from this estimation. The calibrations of Schlegel et al. (1998), and Schlafly & Finkbeiner (2011) give values of 0.037 and 0.032, respectively. We have not attempted a reddening determination from the colour $(V-I)$ being constant between phases 0.5−0.8 for RRab stars (Sturch 1966) and the subsequent calibration of Guldenschuh et al. (2005), since our I light curves are scanty and phase gaps are present. Hence we adopted the value of $E(B-V) = 0.032 \pm 0.002$ from the calibration by Schlafly & Finkbeiner (2011).

7. PHYSICAL PARAMETERS OF THE RR LYRAE STARS FROM THE LIGHT CURVES FOURIER DECOMPOSITION

The Fourier decomposition of the light curves of RR Lyrae stars, both RRab and RRc, is a well established approach towards the determination of some

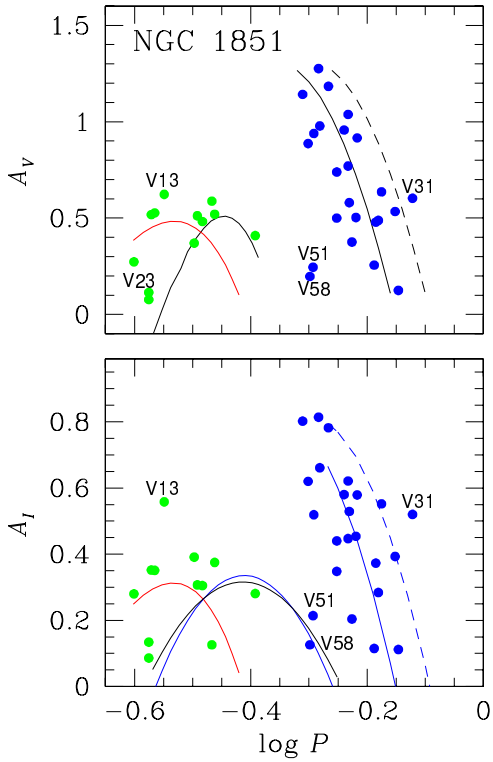

Fig. 4. Period-amplitude diagram for RR Lyrae stars in NGC 1851. Blue and green circles represent RRab and RRc stars, respectively. The colour figure can be viewed online.

physical parameters, mainly the metallicity [Fe/H], the luminosity (or absolute magnitude M_{V} and hence the distance), as well as the mass and mean stellar radius. The Fourier decomposition technique, as well as the semi-empirical calibrations and their zero points leading to the physical parameters, have been presented and discussed in detail in the papers by Arellano Ferro et al. (2010). A summary of the results for 40 clusters calculated homogeneously for over more than a decade can be found in Arellano Ferro (2024). The interested reader is referred to those works for the the involved details.

In the present paper we have limited the calculation of physical parameters to those stars that have proven to be likely cluster members, according to the discussion offered in §4 and summarized in Table 4.

7.1. *Physical Parameters of RR Lyrae Stars*

In Table 5 are given the values of [Fe/H] in the scales of Zinn & West (1984) and in the spectroscopic scale of Carretta et al. (2009) for the member RRab and RRc stars. Also listed are the individual values of $\log T_{\mathrm{eff}}$, $\log(L/L_{\odot})$, $M/M_{\odot}$, $R/R_{\odot}$ and distance. All the reported mean values in this table have been weighted by the inner uncertainties,

TABLE 4

GENERAL DATA OF VARIABLES IN THE FIELD OF NGC 1851[1]

Variable	Type	$<V>$ (mag)	$<I>$ (mag)	A_V (mag)	A_I (mag)	Period (days)	HJD_{max} (d+2450000)	B&C (M/F)	V&B %	Memb. (m/f/?)	RA (J2000.0)	Dec. (J2000.0)
V1	RRab	16.161	15.617	1.276	0.814	0.520583	8581.4671	M1	0.99	m	05:14:28.94	−40:02:56.5
V2	CST	—	—	—	—	—	—	M1	0.99	m	05:14:02.75	−40:02:24.5
V3	RRc	16.068	15.627	0.512	0.307	0.322103	8665.7971	M1	1.00	m	05:14:02.46	−40:01:20.7
V4	RRab	16.197	15.617	0.770	0.447	0.585438	8602.4723	M1	0.99	m	05:14:08.56	−40:02:17.2
V5	RRab	16.015	15.490	0.580	0.529	0.587831	7596.6515	M1	0.99	m	05:14:09.90	−40:02:12.1
V6	RRab	16.094	15.537	0.916	0.579	0.606628	8468.5608	M1	1.00	m	05:14:00.02	−40:03:04.4
V7	RRab	16.151	15.393	1.038	0.621	0.585186	8581.4660	M1	0.99	m	05:14:07.04	−40:04:43.4
V8	RRab	16.154	15.566	0.939	0.519	0.510979	8469.8129	M1	0.16	m	05:14:08.93	−40:02:27.2
V9	L/SR	—	—	—	—	—	—	M1	1.00	m	05:14:01.34	−40:02:06.0
V10	RRab	16.304	15.709	0.887	0.620	0.499528	8468.6287	M1	1.00	m	05:14:10.96	−40:06:09.1
V11	RRab	15.908	15.411	0.636	0.552	0.667919	8581.5263	M1	1.00	m	05:14:12.65	−40:05:07.8
V12	RRab	16.223	15.684	0.957	0.580	0.575942	8586.5057	M1	0.99	m	05:13:59.85	−40:03:41.9
V13	RRc	16.170	16.172	0.623	0.558	0.282543	8580.5020	M1	0.61	?	05:14:06.77	−40:02:07.7
V14	RRab	15.413	14.697	0.376	0.204	0.594038	8469.7261	M1	0.89	m	05:14:12.85	−40:02:34.9
V15	RRab	16.140	15.353	1.184	0.782	0.541344	7002.5754	M1	0.99	m	05:14:09.11	−40:02:01.4
V16	RRab	16.111	15.711	1.142	0.802	0.488699	7380.6230	M1	1.00	m	05:14:12.28	−40:02:52.1
V17	RRab	16.073	15.594	0.534	0.393	0.704841	8467.5715	M1	0.99	m	05:14:02.92	−40:03:50.4
V18	RRc	16.078	15.704	0.527	0.351	0.272094	8467.5579	M1	1.00	m	05:14:09.93	−40:00:13.6
V19	RRc	15.852	15.392	0.409	0.281	0.405181	8602.4853	M1	0.99	m	05:14:08.79	−40:03:25.3
V19	RRc	15.852	15.392	0.409	0.281	0.405181	8602.4853	M1	0.99	m	05:14:08.79	−40:03:25.3
V20	RRab	16.161	15.583	0.739	0.440	0.559460	8467.6636	M1	0.00	m	05:14:05.58	−40:03:17.0
V21	RRc	16.107	15.804	0.518	0.352	0.268520	8581.4671	M1	0.99	m	05:14:01.15	−40:01:53.9
V22	RRab	15.804	15.350	0.500	0.348	0.559401	8602.4613	M1	0.99	m	05:14:17.51	−40:01:00.7
V23	RRc	16.187	15.823	0.114	0.134	0.265835	8469.7203	M1	1.00	m	05:14:16.16	−40:03:47.4
V24	Lb/S	13.161	11.528	—	—	—	—	M1	1.00	m	05:14:19.35	−40:04:23.9
V25	EC	15.706	14.823	0.461	0.445	0.173673	8587.5103	M2	0.00	f	05:13:55.81	−40:07:32.0
V26	RRc	16.149	15.732	0.482	0.305	0.328669	8469.7001	M1	0.99	m	05:13:55.36	−40:01:11.1
V27	RRab	16.063	15.532	0.978	0.661	0.523208	7440.3531	M1	0.99	m	05:14:03.72	−40:03:05.7
V28	RRab	—	—	—	—	—	—	M1	0.99	m	05:14:09.76	−40:03:10.7
V29	RRab	15.671	15.073	0.503	0.454	0.603592	8469.7120	M1	0.55	m	05:14:05.54	−40:02:21.1
V30	RRab	—	—	—	—	—	—	M2	0.90	m	05:14:07.56	−40:02:59.3
V31	RRab	15.973	15.404	0.603	0.520	0.755159	7873.3458	M1	0.99	m	05:14:08.75	−40:03:08.0
V32	RRab	15.909	15.073	0.488	0.284	0.659681	8602.4747	M1	0.99	m	05:14:04.68	−40:02:16.2
V33	RRc	15.680	14.818	0.588	0.126	0.341202	8468.5790	M1	0.99	m	05:14:07.93	−40:03:14.2
V34	RRc	15.989	15.620	0.520	0.375	0.345033	8468.6727	M1	0.83	m	05:14:09.81	−40:03:03.3
V35	RRc	16.137	15.655	0.370	0.391	0.318175	7380.6231	M1	0.99	m	05:14:08.30	−40:02:48.6
V36	RRab	—	—	—	—	—	—	UN	U	?	05:14:07.62	−40:02:42.5
V37	RRc	13.217	11.769	0.066	0.046	0.351040	8469.6989	UN	1.00	f	05:14:07.56	−40:03:07.4
V38	RRab	15.885	0	0.479	0.373	0.653044	8468.7343	M1	0.99	m	05:14:06.77	−40:03:07.0
V39	RRab	—	—	—	—	—	—	M1	0.83	m	05:14:06.64	−40:02:55.9
V40	RRab	—	—	—	—	—	—	M1	0.84	m	05:14:06.50	−40:02:42.3
V41	RRab	—	—	—	—	—	—	UN	U	?	05:14:06.22	−40:02:48.1
V42	RRc	14.648	13.638	0.360	0.163	0.309567	8580.5193	M1	0.20	f	05:14:06.27	−40:02:56.9
V43	RRab	—	—	—	—	—	—	M2	0.99	m	05:14:06.27	−40:02:44.6
V44	RRab	—	—	—	—	—	—	UN	0.13	?	05:14:06.12	−40:02:53.5
V45	RRc	14.640	13.283	0.179	0.123	0.256363	8581.4970	UN	0.94	f	05:14:06.00	−40:02:36.5
V46	RRc	14.637	14.386	0.141	0.303	0.289664	8469.6989	M2	0.98	f	05:14:05.76	−40:02:55.4
V47	RRc	15.629	14.703	0.369	0.148	0.280101	8602.4680	M2	0.59	?	05:14:05.07	−40:02:40.0
V48	RRab	15.176	15.177	0.547	0.220	0.520895	8586.5101	M2	0.15	f	05:14:04.63	−40:03:00.9
V49	RRc	14.174	0	0.077	0.086	0.265827	8468.5790	M1	0.99	m	05:14:04.41	−40:02:56.5
V50	RRc	15.462	14.787	0.231	0.135	0.325064	8581.5275	M1	0.00	f	05:14:03.18	−40:03:23.8
V51	RRab	14.805	13.899	0.245	0.214	0.509389	8580.5303	M1	1.00	m/f?	05:14:02.75	−40:02:24.5
V52	RRab	16.120	15.327	0.256	0.115	0.648831	8468.6052	M1	0.99	m	05:14:02.44	−40:02:33.8
V53	RRc	12.617	11.260	0.260	0.257	0.325140	8581.4789	UN	0.99	f	05:14:06.54	−40:02:49.6
V54	L	—	—	—	—	—	—	M1	0.99	m	05:14:09.12	−40:02:54.8
V55	L	—	—	—	—	—	—	M1	1.00	m	05:14:09.70	−40:03:14.9

which are given between parentheses as described in the notes at the bottom of the table. The average [Fe/H] and distances are considered good representations of the metallicity and distance of the parental cluster. We find $[\mathrm{Fe/H}]_{\mathrm{ZW}} = -1.35 \pm 0.22$, or in the spectroscopic scale of Carretta et al. (2009) $[\mathrm{Fe/H}]_{\mathrm{UV}} = -1.16 \pm 0.25$ and a distance to the cluster of 11.9 ± 0.6 kpc.

TABLE 4. CONTINUED

Variable	Type	$<V>$ (mag)	$<I>$ (mag)	A_V (mag)	A_I (mag)	Period (days)	HJD_{max} (d+2450000)	B&C (M/F)	V&B %	Memb. (m/f/?)	RA (J2000.0)	Dec. (J2000.0)
New Stars Identified in the NGC1851 Field.												
V56	SX Phe?	18.381	17.842	0.273	0.28	0.250666	8468.5802	M1	1.00	m	05:13:41.80	−39:58:52.3
F1	RRc	18.419	17.282	0.236	0.455	0.337433	8467.5760	FS	0.00	f	05:13:43.90	−39:59:10.4
F2	RRc	17.843	16.100	0.236	0.296	0.257364	8467.5660	FS	0.00	f	05:13:44.59	−39:58:55.6
Variables in *Gaia*-DR3 confirmed in the present work												
V57(G3)	RRab	16.106	15.509	0.141	0.122	0.714154	8468.6053	M1	1.00	m	05:13:51.14	−40:02:37.2
V58(G10)	RRab	14.352	13.211	0.197	0.126	0.503017	7063.5570	M1	1.00	m	05:14:07.05	−40:02:18.2
V59(G11)	L	13.55	12.03	0.40	0.21	——	——	M1	1.00	m	05:14:08.96	−40:02:35.0
V60(G13)	L	13.42	11.63	0.37	0.20	——	——	M1	1.00	m	05:14:09.21	−40:02:44.2
V61(G14)	L	13.27	11.62	0.43	0.19	——	——	M1	1.00	m	05:14:07.67	−40:02:30.3
Variables in *Gaia*-DR3 not confirmed in the present work												
		$\overline{V}$	$\overline{I}$									
G1	——	19.129	18.268	——	——	——	——	M1	1.00	m	05:14:02.32	−40:00:01.0
G2	——	18.952	18.593	——	——	——	——	M1	1.00	m	05:13:52.49	−40:01:04.3
G4	——	17.452	16.467	——	——	——	——	M1	1.00	m	05:14:02.37	−40:01:41.9
G5	——	*19.461*	*18.610*	——	——	——	——	M1	1.00	m	05:14:00.84	−40:01:38.4
G6	——	*19.406*	*18.756*	——	——	——	——	M1	1.00	m	05:14:05.02	−40:01:51.9
G7	——	*19.299*	*18.644*	——	——	——	——	M1	1.00	m	05:14:01.50	−40:02:37.9
G8	——	17.027	16.138	——	——	——	——	M1	1.00	m	05:14:08.52	− 40:01:55.8
G9	——	18.585	18.118	——	——	——	——	M2	0.00	f	05:14:11.79	−40:02:09.2
G12	——	13.442	11.815	——	——	——	——	M1	1.00	m	05:14:05.82	−40:02:46.2
G15	——	13.230	11.513	——	——	—-	—-	M1	1.00	m	05:14:07.64	−40:02:27.0
G16	——	*19.629*	*18.943*	——	——	——	——	M2	0.99	m	05:14:02.92	−40:03:30.8
G17	——	16.672	15.754	——	——	——	——	UN	0.89	?	05:14:08.95	−40:03:40.1
G18	——	*19.601*	*18.926*	——	——	——	——	M2	0.01	?	05:14:06.29	−40:03:59.8
G19	——	15.472	14.510	——	——	——	——	M1	1.00	m	05:14:01.95	−40:04:41.6
G20	——	*20.219*	*19.732*	——	——	——	——	M1	1.00	m	05:14:19.10	−40:02:26.4
G21	——	17.363	16.544	——	——	——	——	M2	0.00	?	05:14:13.34	−40:04:12.9

[1]Columns 3 and 4 contain intensity weighted means, except for the LPV stars and for the G-group in the bottom section, which are magnitude weighted means. Numbers in italics are averages exclusively from *Gaia* data transformed into *VI*. Columns 5 and 6 list light curve amplitudes. Column 9 indicates the membership status found in this work from the method of Bustos Fierro & Calderón (2019) (M1 or M2 for likely members, UN for unknown and FS for field stars). Column 10 contains the membership probability assigned by Vasiliev & Baumgardt (2021).

8. THE COLOUR MAGNITUDE DIAGRAM

The observed CMD of NGC 1851 built from our *VI* photometry with only likely cluster member stars was dereddened assuming $E(B-V) = 0.03$ mag. The resulting intrinsic CMD is displayed in Figure 5. All variable stars are plotted with the colours and symbols code in the caption. This diagram helps to confirm the non-membership of many stars, as discussed in previous sections, since their positions are at odds with their variable type in many cases. We remind the reader that our final membership assessment is given Column 11 of Table 4.

We call attention to the distribution of RRab and RRc stars on the HB. Considering exclusively the stars that are clear cluster members, we see that some RRab are located in the bimodal region of the instability strip, i.e. in the intersection of the fundamental and first overtone instability strips. The theoretical bounds of these strips are indicated by the green and blue borders calculated by Bono et al. (1994). The empirical border of the first overtone red edge (FORE) is indicated by the two vertical black lines in the HB (Arellano Ferro et al. 2015, 2016) and matches well with the theoretical FORE. RRab stars crossing to the blue of the FORE are a characteristic of some Oo I type clusters, like NGC 1851, but this does not happen in Oo II clusters, where the RRab remain to the red of the FORE, i.e. off the bimodal region (see Yepez et al. 2022 and references there in for a discussion). This characteristic of Oo II clusters is probably a consequence of the more advanced stage of their evolution to the red, towards the AGB.

Of the 21 stars in the field of NGC 1851 marked in *Gaia*-DR3 as variables, we found a counterpart measured in our photometry for 15 of them. The others, were either too faint or unresolved, given the spatial resolution of our images. For a proper comparison we transformed the *Gaia* photometric data into *VI* using the transformation equations of Riello et al. (2021). We could confirm the variability and variable type of 5 of them; V57-V61 in Table 4. The remaining 10 are plotted in the DCM with purple open triangles and are distributed all across the diagram. The *Gaia* cadence is not designed for the iden-

TABLE 5

PHYSICAL PARAMETERS FROM THE MEMBER RR LYRAE FOURIER LIGHT CURVE DECOMPOSITION

ID	$[Fe/H]_{ZW}$	$[Fe/H]_{UVES}$	M_V	log $T_{\rm eff}$	$\log(L/L_\odot)$	$M/M_\odot$	D(kpc)	$R/R_\odot$
				RRab				
V1	-1.49(3)[1]	-1.40(3)	0.57(1)	3.82(1)	1.68(1)	0.74(7)	12.55(3)	5.42(1)
V6	-1.25(5)	-1.14(4)	0.54(1)	3.81(1)	1.69(1)	0.67(8)	12.35(3)	5.69(1)
V7	-1.40(4)	-1.29(4)	0.53(1)	3.81(1)	1.69(1)	0.68(7)	12.73(3)	5.63(1)
V11	-1.32(34)[2]	-1.20(32)[2]	0.52(1)	3.80(1)	1.70(1)	0.62(11)	11.44(1)	5.85(1)
V12	-1.47(6)	-1.38(7)	0.55(1)	3.81(1)	1.69(1)	0.70(11)	13.00(4)	5.61(2)
V15	-1.43(9)	-1.33(9)	0.61(1)	3.82(2)	1.66(1)	0.68(12)	12.22(6)	5.35(2)
V16	-1.05(6)	-0.94(5)	0.60(1)	3.82(1)	1.66(1)	0.68(9)	12.42(4)	5.07(2)
V38	-1.41(12)	-1.31(12)	0.55(1)	3.84(3)	1.69(1)	0.40(15)	11.34(3)	4.87(1)
Mean	-1.38	-1.25	0.54	3.81	1.68	0.67	11.92	5.52
σ	±0.15	±0.15	±0.03	±0.01	±0.02	±0.11	±0.68	±0.33
				RRc				
V3	-1.56(22)	-1.49(24)	0.57(1)	3.83(1)	1.67(1)	0.78(1)	12.06(3)	4.96(1)
V9	-1.81(29)	-1.82(38)	0.51(1)	3.83(1)	1.70(1)	0.63(1)	11.21(5)	5.23(3)
V21	-0.96(16)	-0.87(11)	0.63(1)	3.88(1)	1.65(1)	0.59(1)	11.95(6)	4.00(1)
V23	-1.45(47)	-1.35(48)	0.75(2)	3.86(1)	1.60(1)	0.63(2)	11.70(12)	4.09(4)
V26	-1.36(21)	-1.25(21)	0.54(1)	3.84(1)	1.68(1)	0.71(1)	12.67(6)	4.85(2)
V34	-1.07(79)	-0.96(61)	0.49(1)	3.86(1)	1.70(1)	0.59(2)	12.04 (8)	4.64(3)
Mean	-1.29	-1.07	0.59	3.85	1.65	0.64	11.96	4.42
σ	±0.31	±0.35	±0.10	±0.02	±0.04	±0.08	±0.48	±0.49

[1]Numbers in parentheses indicate the internal uncertainty expressed to the last digit; e.g. -1.49(3) is equivalent to -1.49±0.03.
[2]Value not included in the mean.

tification of some variables; therefore, the authenticity of these variables will have to be confirmed with proper time-series observations on images of resolution higher than ours.

The theoretical ZAHB shown in the figure as a red continuous locus was calculated by Yepez et al. (2022) using the models built with the Eggleton code (Pols et al. 1997, 1998; Schröder et al. 1997) for a metallicity of z=0.001, a core mass of 0.5 $M/M_\odot$, and a range of total masses of 0.59-0.68 $M/M_\odot$. The isochrone is from VandenBerg et al. (2014) for [Fe/H]=−1.35 and an age of 12.0 Gyr.

All the above loci have been drifted to a distance of 11.95 kpc and represent well the observed distribution of the cluster member stars.

9. CONCLUSIONS

The presence of variable field stars projected against a Galactic globular cluster is very common, and while such contamination by field stars in the Galactic bulge globular clusters can be remarkably high (e.g. see the case of NGC 6558 Arellano Ferro et al. 2024) due to the richness of the bulge of field variable stars, particularly of RR Lyrae, it can also be noticeable in more isolated globular clusters in the outer regions of the Milky Way. Such is the case of NGC 1851, as we have demonstrated in the present work. An *ad hoc* membership analysis based on the proper motions and parallaxes available in *Gaia*-DR3, complemented with mean magnitudes and colours in the $V-(V-I)$ CMD, has shown that of the 55 variables originally listed in the CVSGC, 8 have been found to be clearly field stars, and for 6 more the membership cannot be solidly assessed due to the lack of proper motion data or to blending with bright neighbours, particularly in the central regions of the cluster.

Three variables not detected before were identified, but only one turned out to be a cluster member. We named it V56 and classified it tentatively as an SX Phe star. Among the 21 variables reported by *Gaia* not included in the CVSGC, we confirmed the variability of two RRab and three long term L variables. Since they turned out to be cluster members we assign to them variable names V57-V61.

Identifying variable cluster members is rewarding, since they can be used with confidence, as indicators of average physical quantities representative of the parental cluster. Here we estimated the mean

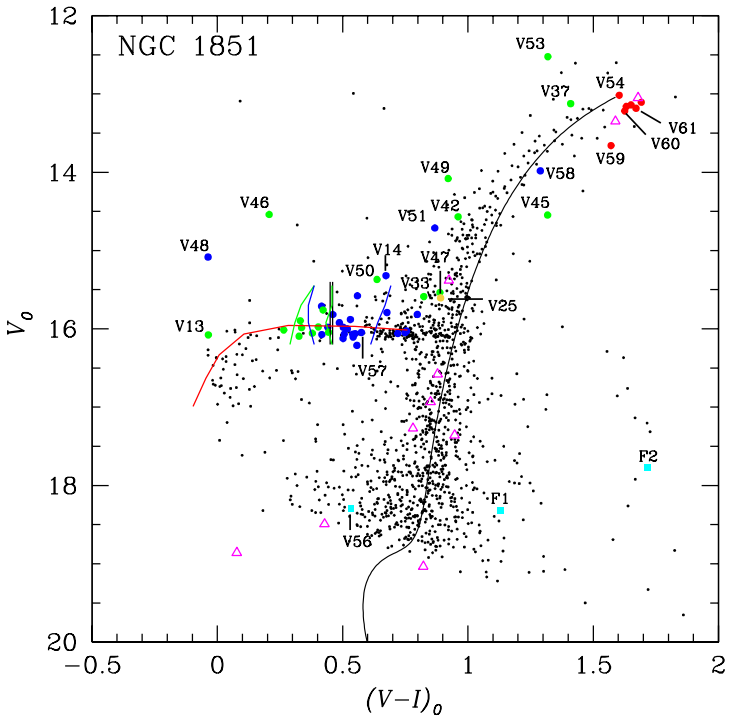

Fig. 5. Color-Magnitude Diagram (CMD) of NGC 1851. Variables stars in the field of the cluster are plotted with colour symbols according to the following code:solid blue and green circles represent RRab and RRc star respectively; red circles are for SR/L variables near the tip of the RGB. The star V25, classified as an eclipsing binary, is shown with a yellow circle. Turquoise colour is use for three newly identified variables, and purple open triangles for variables reported in *Gaia* that were not identified in our photometry or were not confirmed as variables. The Red ZAHB was constructed by Yepez et al. (2022) using the models built from with the Eggleton (Pols et al. 1997, 1998; Schröder et al. 1997). The green and blue vertical nearly vertical lines on the HB are the theoretical first overtone and fundamental mode instability strips respectively (Bono et al. 1994).en The isochrone is from VandenBerg et al. (2014) for [Fe/H]=-1.35 and an age of 12.0 Gyrs. The vertical black lines at the ZAHB mark the empirical red edge of the first overtone instability strip (Arellano Ferro et al. 2015, 2016). The colour figure can be viewed online.

metallicity and distance of NGC 1851 via the Fourier decomposition of RR Lyrae light curves, to find $[\mathrm{Fe/H}]_{\mathrm{ZW}} = -1.35 \pm 0.22$ dex and $d = 11.9 \pm 0.6$ kpc.

A few comments on the position of NGC 1851 relative to the Oosterhoff gap are in order, since the cluster has been associated with an CMa dwarf galaxy (Martin et al. 2004). We noted before that the average period of the member RRab stars is $<P\mathrm{ab}> = 0.57 \pm 0.06$ d, which with the metallicity $[\mathrm{Fe/H}]_{\mathrm{ZW}} = -1.35$ places the cluster among the Oo I clusters and slightly off the Oosterhoff gap marked by Catelan (2009, see his Figure 5). On the other hand, let us consider the structural, or horizontal branch type parameter, defined as $HBt = (B - R)/(B + V + R)$, Lee et al. (1994), where B and R are the number of stars to the blue and to the red of the instability strip respectively, and V represents the number of RR Lyrae in the instability strip (Lee et al. 1994; Demarque et al. 2000). In the [Fe/H]-HBt plane Catelan (2009, his Figure 7) identified a region devoid of Galactic globular clusters, but populated otherwise by clusters associated with neighbouring galaxies, and termed this region as "forbidden" or as the "Oosterhoff gap". We should recall here that the Oo I clusters NGC 1851 and NGC 2808, as well as the Oo II clusters NGC 2298 and NGC 1904, have been suggested by Martin et al. (2004) to be associated to the Canis Major dwarf galaxy accreted by the Milky Way. More recently, Callingham et al. (2022) have associated the first three to the Gaia-Enceladus-Sausage merger event and to the Helmi merger (Helmi et al. 2018) for the case of NGC 1904.

NGC 1851 and NGC 2808 have well developed HB blue tails but prominent red clumps; hence their HBt values are very red, i.e. negative, whereas NGC 1904 and NGC 2298 have massive blue tails

but lack a red clump. Therefore, their HBt values are very blue, hence large and positive.

Considering the updated version of the [Fe/H]-HBt plane (Yepez et al. 2022, see their Figure 11), and plotting these four clusters with the coordinates ([Fe/H],HBt); NGC 1851 (−1.35,−0.36, this work), NGC 2808 (−1.15, −0.49, Catelan 2009), NGC 1904 (−1.68,+0.74, Arellano Ferro 2024) and NGC 2298 (−1.96,+0.96, Torelli et al. 2019), it is evident that none of these four clusters occupy the Oosterhoff gap.

We are faced with two possible conclusions; these clusters are not associated to external galaxy mergers of the MW beyond the spatial coincidence, or else the globular clusters of extragalactic origin can occupy regions in the [Fe/H]-HBt or [Fe/H]-$< P_{\rm ab} >$ planes other than the Oosterhoff gap defined by Catelan (2009), as in fact some are seen in his Figures 5 and 7. This reinforces the view that the Oosterhoff gap retains its meaning only in Galactic terms. Hence, we do not find compelling evidence, from these arguments, for an association of NGC 1851 (and perhaps neither of NGC 2808, NGC 1904 and NGC 2298) to the large accretion events that seem to have sculpted the Galactic halo.

AAF is grateful to the European Southern Observatory (Garching), for warm hospitality during the writing of this work. The permanent support from the IA-UNAM librarian, Beatriz Juárez Santamaría, with the bibliographical material needed for this work is fully acknowledged. AAF also thankfully acknowledges the sabbatical support granted by the program PASPA of DGAPA-UNAM. We have benefited from the support of DGAPA-UNAM through Projects IG100620 and IN103024.

APPENDICES

A. LIGHT CURVES OF THE MEASURED VARIABLE STARS

The light curves of all variables resolved in our photometry are displayed in Figures 6, 7, 8, 9 and 10 for the RRab, RRc, RGBs, newly detected variables and confirmed *Gaia* variables, respectively.

B. COMMENTS ON INDIVIDUAL STARS

V13. This RRc star falls too far to the blue of the HB. Its membership to the the cluster is controversial. The assignment by the B&C membership method and the membership probability assigned by V&B is contradictory. In the period-amplitude diagram the star has too large an amplitude for its period.

V25. In spite of being an eclipsing binary EC, its light curve is included in Figure 7. The only difference with other RRc stars is that its period is much shorter, 0.173673 d, and it is brighter than the HB by about half a magnitude (see CMD of Figure 5), The V light curve exhibits a small flattening near maximum which may be a suggestion of an incipient secondary eclipse. This is also seen in the I-band light curve from the BA19 season.

V34. This variable was first reported by Sumerel et al. (2004) as an RRab star with a period of 0.515 d, which in fact produces a well phased light curve. However, at the coordinates given in the CVSGC we in fact find a variable star, but we find a period of 0.345033 d that displays a clear and complete RRc-like light curve (see Figure 7). The only reason we find for this discrepancy is that the data of Sumerel et al. (2004) cover only about half a cycle, and then their period and type may be spurious. We classified the star as RRc.

V51. It was reported as variable by Sumerel et al. (2004), and the light curve obtained by these authors (labeled NV18), although incomplete, clearly suggests the RRab nature of the star. It was noticed by Layden et al. (2010) that the star is in fact an RR Lyrae stars badly blended with a non-variable star previously identified as V2 by Sawyer (1939). The light curve measured by Layden (2010) was not published, but it was said to be noisy, likely due to the contamination of the brighter V2. Our light curve in Figure 6 is fairly complete, and confirms the RRab nature of the star nicely phased with a period of 0.509389 days. The mean VI magnitude level of our curve is spurious due to the light contamination of V2 and its position in the CMD of Figure 5.

V52. This star is not classified in the present edition of the CVSGC, where only its X-Y coordinates are listed. We have identified the star and found it to be a cluster member RRab star. It sits on the HB and its light curve is properly phased with a period of 0.648831 d.

V56. This is a newly identified variable in this work. Its light curve shape and position on the CMD diagram remind us of an SX Phe-type star. However a period of 0.25 d. is perhaps a little too long for an SX Phe. We have retained it in our general Table 4 as SX Phe? awaiting a confirmation in the future.

V58. Its light curve is that of an RRab; however, it appears about two magnitudes above the HB near the RGB. Both membership approaches, B&C and V&B, based on its proper motion, identify the star as a cluster member. In the identification chart we see that evidently the star is blended with at least

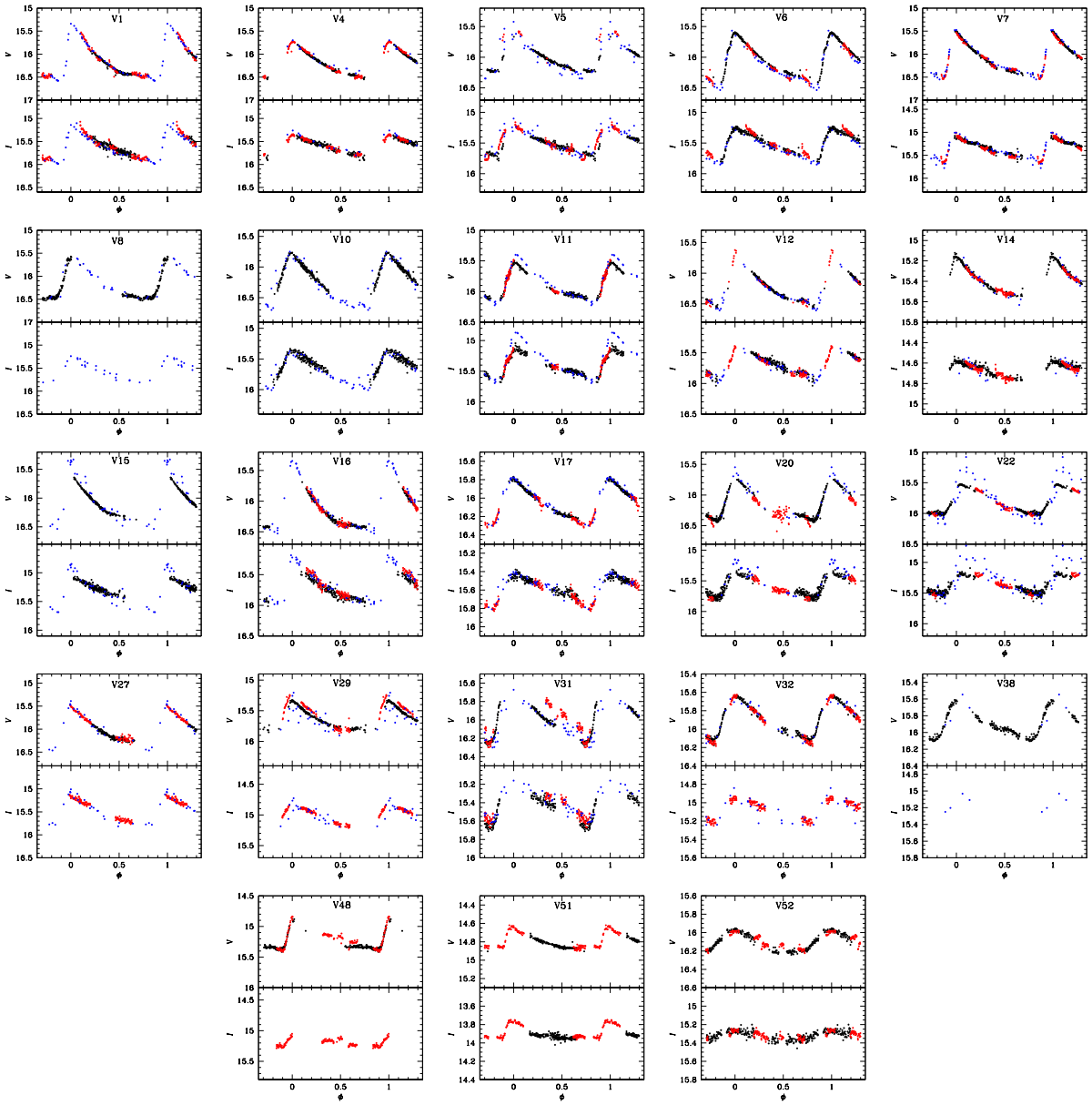

Fig. 6. NGC 1851 RR Lyrae stars *VI* light curves. The colour code is: black: BA18; red: BA19; blue: *Gaia*-DR3. The colour figure can be viewed online.

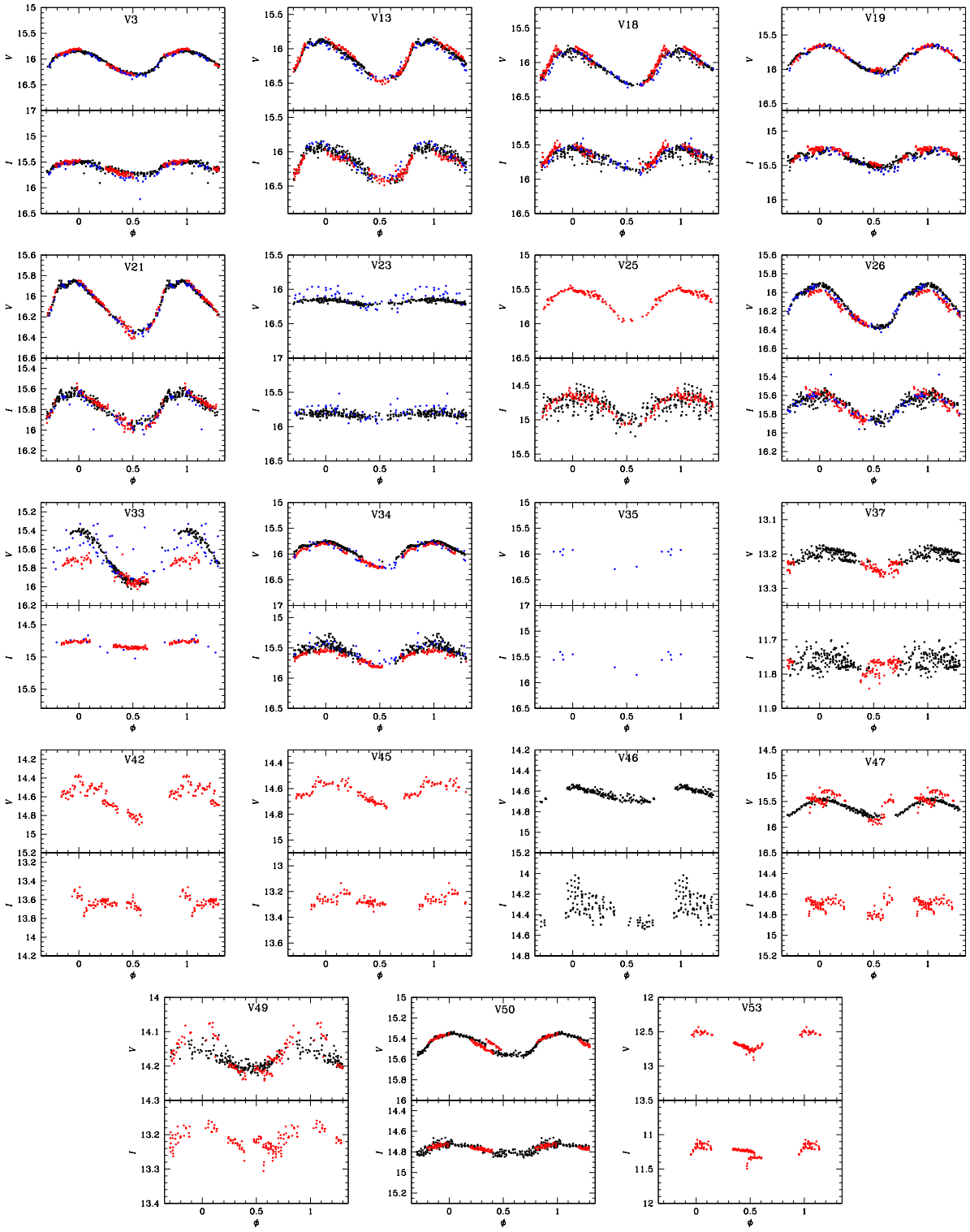

Fig. 7. Light curves of the RRc stars in the field of NGC 1851. The colour code is as in Figure 6. The colour figure can be viewed online.

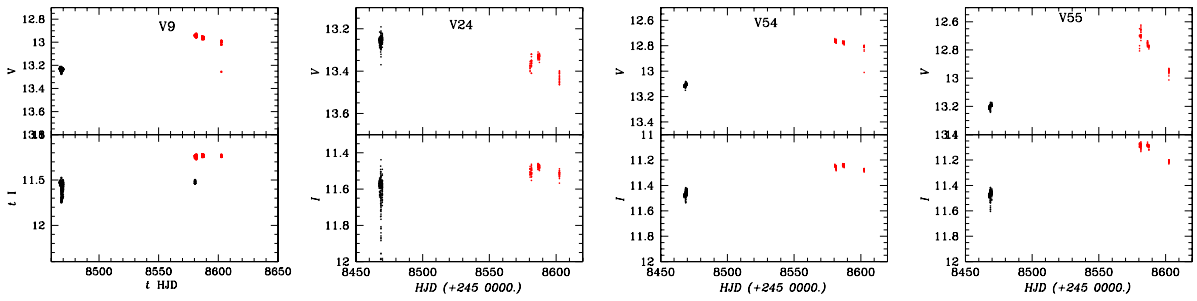

Fig. 8. Light curves of long-period variables in NGC 1851 plotted as a function of heliocentric Julian date (HJD). Colour coding follows that of Figure 6. The colour figure can be viewed online.

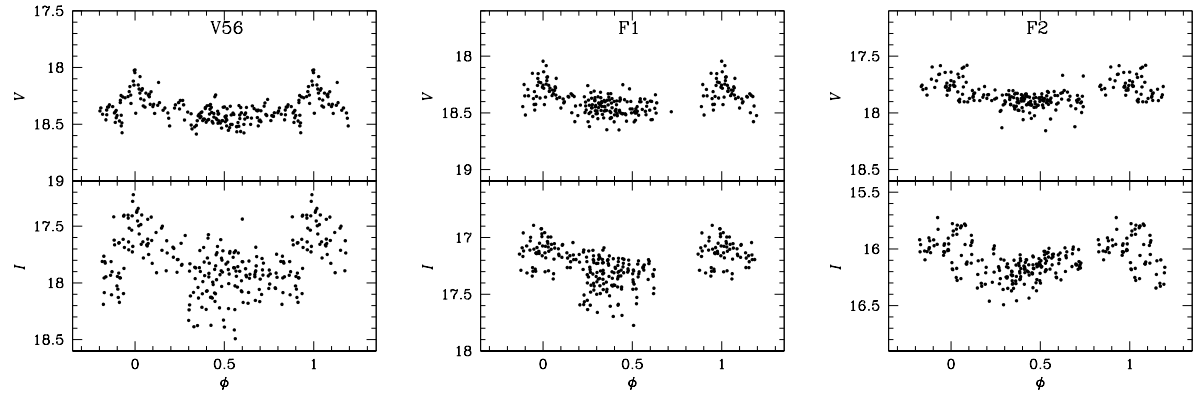

Fig. 9. Newly identified variable stars not previously recorded.They have been phased with the periods in Table 4.

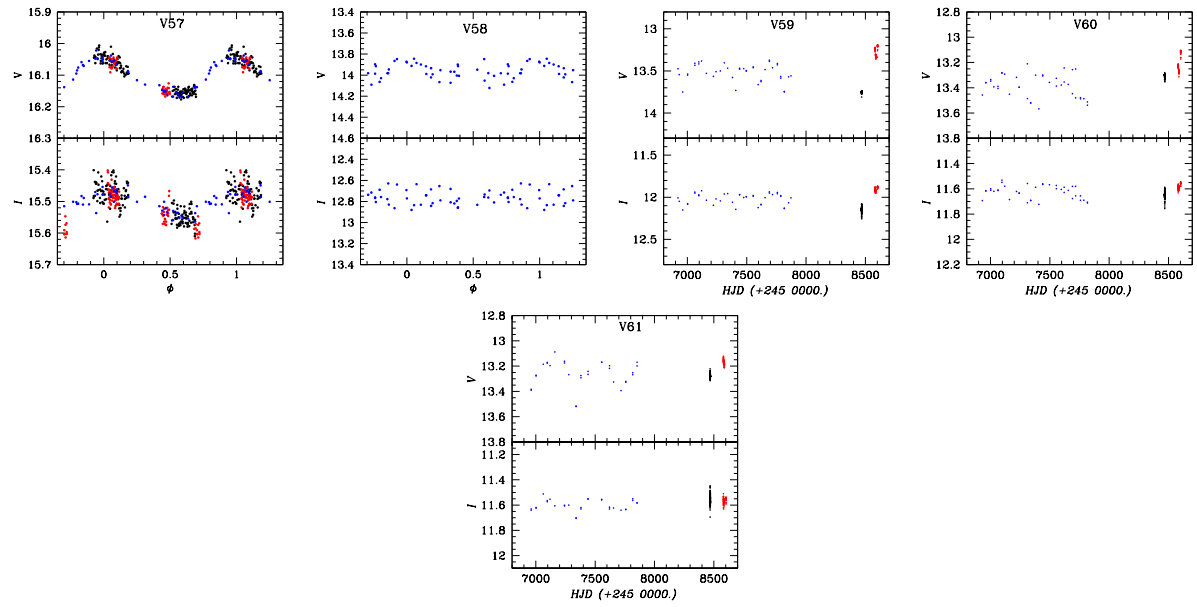

Fig. 10. Light curves of the confirmed variables reported in *Gaia*-DR3. Colour code as in Figure 6. The colour figure can be viewed online.

a brighter star, which explains its mean magnitude being spuriously too bright. We have considered the star to be a cluster member and assigned to it the variable name V58.

REFERENCES

Arellano Ferro, A. 2024, IAUS 376, At the crossroads of astrophysics and cosmology: Period-luminosity relations in the 2020s, ed. R. De Grijs, P. A. Whitelock, and M. Catelan (CUP), 222, https://doi.org/10.1017/S1743921323002880

Arellano Ferro, A., Giridhar, S., & Bramich, D. M. 2010, MNRAS, 402, 226, https://doi.org/10.1111/j.1365-2966.2009.15931.x

Arellano Ferro, A., Luna, A., Bramich, D. M., et al. 2016, Ap&SS, 361, 175, https://doi.org/10.1007/s10509-016-2757-5

Arellano Ferro, A., Mancera Piña, P. E., Bramich, D. M., et al. 2015, MNRAS, 452, 727, https://doi.org/10.1093/mnras/stv1299

Arellano Ferro, A., Zerpa Guillen, L. J., Yepez, M. A., et al. 2024, MNRAS, 532, 2159, https://doi.org/10.1093/mnras/stae1609

Belokurov, V., Erkal, D., Evans, N. W., Koposov, S. E., & Deason, A. J. 2018, MNRAS, 478, 611, https://doi.org/10.1093/mnras/sty982

Bono, G., Caputo, F., & Stellingwerf, R. F. 1994, ApJ, 423, 294, https://doi.org/10.1086/173806

Bramich, D. M. 2008, MNRAS, 386, 77, https://doi.org/10.111/j.1745-3933.2008.00464.x

Bramich, D. M., Bachelet, E., Alsubai, K. A., Mislis, D., & Parley, N. 2015, A&A, 577, 108, https://doi.org/10.1051/0004-6361/201526025

Bramich, D. M., Horne, K., Albrow, M. D., et al. 2013, MNRAS, 428, 2275, https://doi.org/10.1093/mnras/sts184

Bustos Fierro, I. H. & Calderón, J. H. 2019, MNRAS, 488, 3024, https://doi.org/10.1093/mnras/stz1879

Callingham, T. M., Cautun, M., Deason, A. J., et al. Frenk, C. S., Grand, R. J. J., & Marinacci, F. 2022, MNRAS, 513, 4107, https://doi.org/10.1093/mnras/stac1145

Carballo-Bello, J. A., Martínez-Delgado, D., Navarrete, C., et al. 2018, MNRAS, 474, 683, https://doi.org/10.1093/mnras/stx2767

Carretta, E., Bragaglia, A., Gratton, R., D'Orazi, V., & Lucatello, S. 2009, A&A, 508, 695, https://doi.org/10.1051/0004-6361/200913003

Catelan, M. 2009, Ap&SS, 320, 261, https://doi.org/10.1077/s10509-009-9987-8

Clement, C. M., Muzzin, A., Dufton, Q., et al. 2001, AJ, 122, 2587, https://doi.org/10.1086/323719

Demarque, P., Zinn, R., Lee, Y.-W., & Yi, S. 2000, AJ, 119, 1398, https://doi.org/10.1086/301261

Gaia Collaboration, Vallenari, A., Brown, A. G. A., et al. 2023, A&A, 674, 1, https://doi.org/10.1051/0004-6361/202243940

Guldenschuh, K. A., Layden, A. C., Wan, Y., et al. 2005, PASP, 117, 721, https://doi.org/10.1086/431178

Harris, W. E. 1996, AJ, 112, 1487, https://doi.org/10.1086/118116

Helmi, A., Babusiaux, C., Koppelman, H. H., et al. 2018, Nature, 563, 85, https://doi.org/10.1038/s41586-018-0625-x

Koleva, M., Prugniel, P., Ocvirk, P., Le Borgne, D., & Soubiran, C. 2008, MNRAS, 385, 1998, https://doi.org/10.1111/j.1365-2966.2008.12908.x

Kuzma, P. B., Da Costa, G. S., & Mackey, A. D. 2018, MNRAS, 473, 2881, https://doi.org/10.1093/mnras/stx2353

Landolt, A. U. 1992, AJ, 104, 340, https://doi.org/10.1086/116242

Layden, A. C., Broderick, A. J., Pohl, B. L., et al. 2010, PASP, 122, 1000, https://doi.org/10.1086/656018

Lee, Y.-W., Demarque, P., & Zinn, R. 1994, ApJ, 423, 248, https://doi.org/10.1086/173803

Marino, A. F., Milone, A. P., Yong, D., et al. 2014, MNRAS, 442, 3044, https://doi.org/10.1093/mnras/stu1099

Martin, N. F., Ibata, R. A., Bellazzini, M., et al. 2004, MNRAS, 348, 12, https://doi.org/10.1111/j.1365-2966.2004.07331.x

Pols, O. R., Schröder, K.-P., Hurley, J. R., Tout, C. A., & Eggleton, P. P. 1998, MNRAS, 298, 525, https://doi.org/10.1046/j.1365-8711.1998.01658.x

Pols, O. R., Tout, C. A., Schroder, K.-P., Eggleton, P. P., & Manners, J. 1997, MNRAS, 289, 869, https://doi.org/10.1093/mnras/289.4.869

Riello, M., De Angeli, F., Evans, D. W., et al. 2021, A&A, 649, 3, https://doi.org/10.1051/0004-6361/202039587

Sawyer, H. B. 1939, PDDO, 1, 125

Schlafly, E. F. & Finkbeiner, D. P. 2011, ApJ, 737, 103, https://doi.org/10.1088/0004-637X/737/2/103

Schlegel, D. J., Finkbeiner, D. P., & Davis, M. 1998, ApJ, 500, 525, https://doi.org/10.1086/305772

Schröder, K.-P., Pols, O. R., & Eggleton, P. P. 1997, MNRAS, 285, 696, https://doi.org/10.1093/mnras/285.4.696

Stetson, P. B. 2000, PASP, 112, 925, https://doi.org/10.1086/316595

Sturch, C. 1966, ApJ, 143, 774, https://doi.org/10.1086/148557

Sumerel, A. N., Corwin, T. M., Catelan, M., Borissova, J., & Smith, H. A. 2004, IBVS, 5533, 1

Torelli, M., Iannicola, G., Stetson, P. B., et al. 2019, A&A, 629, 53, https://doi.org/10.1051/0004-6361/201935995

VandenBerg, D. A., Brogaard, K., Leaman, R., & Casagrande, L. 2013, ApJ, 775, 134, https://doi.org/10.1088/0004-637X/775/2/134

Vasiliev, E. & Baumgardt, H. 2021, MNRAS, 505, 5978, https://doi.org/10.1093/mnras/stab1475

Walker, A. R. 1998, AJ, 116, 220, https://doi.org/10.1986/300432
Yepez, M. A., Arellano Ferro, A., Deras, D., et al. 2022, MNRAS, 511, 1285, https://doi.org/10.1093/mnras/stac054
Zhang, T., Ramakrishnan, R., & Livny, M. 1996, ACM SIGMOD Recoed, 25, 103, https://doi.org/10.1145/235968.233324
Zinn, R. & West, M. J. 1984, ApJS, 55, 45, https://doi.org/10.1086/190947

A. Arellano Ferro: Instituto de Astronomía, Universidad Nacional Autónoma de México, Ciudad Universitaria, C.P. 04510, México.
C. E. Pérez Parra and L. J. Zerpa Guillen: Universidad de Los Andes, Facultad de Ciencias, Dpto. Física, Grupo de Astrofísica Teórica, Mérida, Venezuela.
C. E. Pérez Parra and L. J. Zerpa Guillen: Fundación Centro de Investigaciones de Astronomía Francisco, J. Duarte (CIDA), Mérida, Venezuela.
I. Bustos Fierro: Observatorio Astronómico, Universidad Nacional de Córdoba, Córdoba C.P. 5000, Argentina.
Z. Prudil: European Southern Observatory, , Karl-Schwarzschild-Strasse 2, 85748, Garching, Germany.
M. A. Yepez: Instituto Nacional de Astrofísica, Óptica y Electrónica (INAOE), Luis Enrique Erro No.1, Tonantzintla, Puebla, C.P. 72840, México.
M. A. Yepez: Consejo Nacional de Humanidades, Ciencias y Tecnologías, Av. Insurgentes Sur 1582, 03940, Ciudad de México, México.